One-Step Preparation of Antireflection Film by Spin-Coating of Polymer/Solvent/Nonsolvent Ternary System

Min Soo Park, Youngmin Lee, and Jin Kon Kim*

National Creative Research Center for Block Copolymer Self-Assembly, Department of Chemical Engineering and Polymer Research Institute, Electric and Computer Engineering Division, Pohang University of Science and Technology, Kyungbuk 790-784, Korea

Received January 13, 2005. Revised Manuscript Received May 21, 2005

An antireflection film was prepared by spin-coating of poly(methyl methacrylate) (PMMA) solution in chloroform in the presence of small amounts of nonsolvent alkanes. When the vapor pressure of a nonsolvent was lower than that of chloroform, a dense skin layer was formed because of the rapid solvent evaporation during spin-coating, whereas increasing the nonsolvent content below this layer resulted in a phase-separated structure. The phase-separated structure below the dense skin layer became a porous layer after the complete evaporation of both chloroform and nonsolvent. Since the film thickness after spin-coating was on the order of hundreds of nanometers, the size of the pores formed at the inner layer was also a few hundred nanometers. The two layers consisting of a dense skin layer and an inner porous layer exhibited excellent antireflection (AR) when coated on glass substrate. By a one-step procedure of spin-coating of PMMA, the film has high transmittance of over 98% at visible wavelengths. Furthermore, due to the dense skin layer in this AR film, an additional spin-coating could be easily performed on this film.

I. Introduction

Antireflection (AR) coatings have been widely employed in optical and optoelectronic materials.[1−6] A decrease in light reflection, and thus an increase in the transmittance of light, enables clear viewing with the eyes of glass and displaying surfaces.[2] The principle of AR coating is based on the destructive interference of reflected light from interfaces between air and a film, one film and another film in the case of multilayered film coating, or a film and the substrate. In the case of a one-layer coating, two criteria should be met: a film thickness of a quarter wavelength and a refractive index (n) intermediate between those of air and the substrate. For complete zero-reflectance, the refractive index of the AR coating layer should have the geometric mean value of the refractive indices of air and the substrate.[1] For a glass substrate ($n = 1.52$), a film with $n = 1.23$ gives zero-reflectance at a specific wavelength. Even though the refractive index of magnesium fluoride ($n = 1.38$) is the lowest among inorganic materials at visible wavelengths,[1] this value is still large for the zero-reflectance condition. Fluoropolymers with $n \sim 1.34$ have been used for AR coating, but these have limitations due to the lack of suitable solvent and high melting temperature, in addition to high price.[7]

AR coating has usually been achieved by using inorganic materials with the closest refractive index to the desired value or porous structures whose sizes are small enough not to cause light scattering.[1,8−11] An etched glass surface[8] is used as a porous layer with lower refractive index than bulk glass. The sol−gel process[9] and randomly deposited particles[10,11] could act as porous layers. In nature, a moth's eye structure[12] is an excellent AR layer. Recently, polymer materials[13−16] have been used for the AR coating layer because of easy and economic processing compared with inorganic materials. Also, they are easily coated on large areas and flexible substrates. Steiner and co-workers[13] used nanophase-separated film prepared by polystyrene (PS) and poly(methyl methacrylate) (PMMA) blend followed by selective etching of the PS phase. Rubner and co-workers[14] used a polyelectrolyte multilayer film consisting of poly(allylamine hydrochloride) and poly(acrylic acid) that undergo a reversible pH-induced swelling transition. A nanoporous structure can be erased and reconstructed by cycling pH. Ibn-Elhaj et al.[15]

* To whom correspondence should be addressed. Fax: +82-54-279-8298. E-mail: jkkim@postech.ac.kr.

(1) Macleod, H. A. *Thin-Film Optical Filters*; Hilger: Bris-tol, UK, 1986.
(2) Nakamura, K.; Matsunaga, N.; Arai, T.; Otani, S.; Yamazaki, H.; Hokazono, H. US Patent 6,502,943, 2003.
(3) Bilyalov, R.; Stalmans, L.; Poortmans, J. *J. Electchem. Soc.* **2003**, *150*, G216.
(4) Saito, S.; Suto, K.; Kimur, T.; Nishizawa, J. *IEEE. Photon. Technol. Lett.* **2004**, *16*, 395.
(5) Tseng, C. L.; Youh, M. J.; Moore, G. P.; Hopkins, M. A.; Stevens, R.; Wang, W. N. *Appl. Phys. Lett.* **2003**, *83*, 3677.
(6) Kanamori, Y.; Ishimori, M.; Hane, K. *IEEE. Photon. Technol. Lett.* **2002**, *14*, 1064.
(7) Castner, D. G.; Grainger, D. W.; Pellerite, M.; Anton, D. *Fluorinated Surfaces, Coatings, and Films*; Oxford University Press: New York, 2001.
(8) Minot, M. J. *J. Opt. Soc. Am.* **1976**, *66*, 515.
(9) Thomas, M. *Appl. Opt.* **1992**, *31*, 6145.
(10) Hattori, H. *Adv. Mater.* **2001**, *13*, 51.
(11) Zhang, X.; Sato, O.; Tauchi, M.; Einaga, Y.; Murakami, T.; Fujishima, A. *Chem. Mater.* **2005**, *17*, 696.
(12) Clapham, P. B.; Hutley, M. C. *Nature* **1973**, *244*, 281.
(13) Walheim, S.; Schäffer, E.; Mlynek, J.; Steiner, U. *Science* **1999**, *283*, 520.
(14) Hiller, J.; Mendelsohn, J. D.; Rubner, M. F. *Nat. Mater.* **2002**, *1*, 59.
(15) Ibn-Elhaj, M.; Schadt, M. *Nature* **2001**, *410*, 796.
(16) Koo, H. Y.; Yi, D. K.; Yoo, S. J.; Kim, D. *Adv. Mater.* **2004**, *16*, 274.

10.1021/cm0500758 CCC: $30.25
Published on Web 06/18/2005

prepared an AR film with nanocorrugated surface topology by irradiating UV onto the blend consisting of photo-cross-linkable prepolymer and monomeric liquid crystal. During UV irradiation, prepolymer becomes a high molecular weight polymer and phase-separates from monomeric liquid crystal, which is removed by selective etching. Kim and co-workers[16] developed the AR coating layer by using a snowman structure of polystyrene particles where smaller particles are located on the bigger particles. However, the above-mentioned AR coating techniques need multiple steps for the film preparation or post-treatment such as etching. Furthermore, these AR films have a porous surface on the top of the film; thus, an additional spin-coating would not be easily performed.

On the other hand, a dense skin layer, once it is formed on the top of the film, can act as a simple protective layer, which allows further coating. Here, we introduce a simple method for the preparation of the AR film by spin-coating of a polymer/solvent/nonsolvent ternary system. This film consists of a dense skin layer and an inner porous layer. Such a ternary system has long been employed for the preparation of separation membrane.[17−24] However, the inner porous layer of a conventional membrane prepared by the ternary system contains pores with a few microns in size that cannot be applied to an optical film.

We controlled the pore sizes of the inner layer down to a few hundreds nanometers by using spin-coating of poly(methyl methacrylate) (PMMA) solution in chloroform in the presence of small amounts of nonsolvent alkanes. When the vapor pressure of the nonsolvent was lower than that of chloroform, a dense skin layer was formed due to the rapid preferential solvent evaporation during spin-coating. At the same time, the nonsolvent content in the inner layer below the dense skin layer increased, and the inner layer became phase-separated from the polymer. The nonsolvent-rich phase becomes porous after complete evaporation of solvent and nonsolvent. We found that the two layers consisting of a dense skin layer and an inner porous layer exhibited excellent antireflection when coated on glass substrate. By one-step preparation of the film on glass by spin-coating, the film exhibited a high transmittance of over 98% at visible wavelengths.

II. Experimental Section

PMMA with a weight-average molecular weight (M_w) of 540 000 and a polydispersity of 2.19 was purchased from SP[2] company. Chloroform was used as a solvent, whereas alkanes with various carbon numbers [six (hexane) to 13 (tridecane)] were used as nonsolvent. Various compositions of polymer/solvent/nonsolvent at a concentration of 0.009 g/cm^3 were spin-coated on both sides of glass substrate to measure transmittance. The film thickness of spin-coated PMMA film was measured with atomic force microscopy (AFM, Nanoscope III, Digital Instrument Co.) after the film was scratched by a razor (see the Supporting Information).

On the other hand, to measure reflectance, one-side of the glass substrate was spin-coated with PMMA solution and the other side was sealed by black tape to eliminate backside reflection. Glass slides, purchased from Corning Glass Works [CORNING brand, Plain (Product #2947)], were soda lime glass with $n \sim 1.52$. Light transmittance and reflectance were measured by UV−vis−NIR spectrophotometer (Cary 5000, Varian Co.). Total reflectance was measured with integrating sphere (Internal DRA-2500, Varian Co.). The characteristic matrix theory[1] was used for model fitting of transmittance and reflectance, assuming that no scattering and absorption were involved.

Morphologies of spin-coated films were investigated by field emission scanning electron microscopy (FE-SEM; Hitachi S-4200). To measure the morphology of the bottom of the spin-coated film, we used a silicon wafer with 200 nm of the sacrificial layer of SiO_2. After PMMA film was spin-coated on this silicon wafer, the film was floated onto water by dissolving the SiO_2 layer by 5 vol % of HF aqueous solution.[25] We assumed that bottom morphologies of PMMA films spin-coated on glass were not different from those spin-coated on the silicon wafer, since top and cross-sectional views for these two films are identical. Amorphous fluoropolymer (AF) [Teflon AF(1600)] was purchased from Dupont Co. A solution of AF 0.003 g/cm^3 in a perfluorinated solvent (Fluorinert FC77, 3M Co.) was spin-coated at 2000 rpm onto the two-layer structured PMMA AR film.

III. Results and Discussion

Figure 1 gives the transmittance and reflectance of glasses spin-coated on both sides from PMMA solution (0.009 g/cm^3) in chloroform with 2 vol % of nonane at three rotating speeds (rpm). The boiling points of chloroform and nonane are 61 and 151 °C, respectively, and the vapor pressures at 25 °C of these two are 26.2 and 0.57 kPa, respectively. As seen in Figure 1, the transmittance of glasses spin-coated on both sides with PMMA considerably increased compared to the glass. At 9000 rpm, very high transmittance (and very low reflectance) was observed at wavelengths of visible light. The maximum transmittance (and the minimum reflectance) is 98.5% (0.84%) at 550 nm. The maximum transmittance (and the minimum reflectance) of a film prepared at 5000 rpm is 99.2% (0.43%) at 710 nm, while that of another film prepared at 3000 rpm becomes 99.0% (0.53%) at 800 nm.

The wavelengths at which transmittances (and reflectances) have their maxima (or minima) increased with increasing film thickness (or decreasing rotating speed). This result can be explained by considering quarter wavelength thickness design of one layer AR coating, $\lambda_o = 4nd$, where n, d, and λ_o are the refractive index, the thickness of the film, and the wavelength, respectively.

The thicknesses of PMMA films measured by AFM at three rotating speeds (9000, 5000, and 3000 rpm) were 80, 101, and 111 nm, respectively (see Supporting Information). For a PMMA film with a thickness of 80 nm, the maximum

(17) Erbil, H. Y.; Demirel, A. L.; Avci, Y.; Mert, O. *Science* **2003**, *299*, 1377.
(18) Park, M. S.; Kim, J. K. *Langmuir* **2004**, *20*, 5347.
(19) Pinnau, I.; Koros, W. J. *J. Appl. Polym. Sci.* **1991**, *43*, 1491.
(20) Pinnau, I.; Koros, W. J. *J. Membr. Sci.* **1992**, *71*, 81.
(21) Niwa, M.; Kawakami, H.; Kanamori, T.; Shinbo, T.; Kaito, A.; Nagaoka, S. *J. Membr. Sci.* **2004**, *230*, 141.
(22) Nakajima, K.; Nagaoka, S.; Kawakami, H. *Polym. Adv. Technol.* **2003**, *14*, 433.
(23) Niwa, M.; Kawakami, H.; Kanamori, T.; Shinbo, T.; Kaito, A.; Nagaoka, S. *Macromolecules* **2001**, *34*, 9039.
(24) Kawakami, H.; Mikawa, M.; Nagaoka, S. *J. Membr. Sci.* **1997**, *137*, 241.
(25) Jeong, U.; Kim, H. C.; Rodriguez, R. L.; Tsai, I. Y.; Stafford, C. M.; Kim, J. K.; Hawker, C. J.; Russell, T. P. *Adv. Mater.* **2002**, *14*, 274.

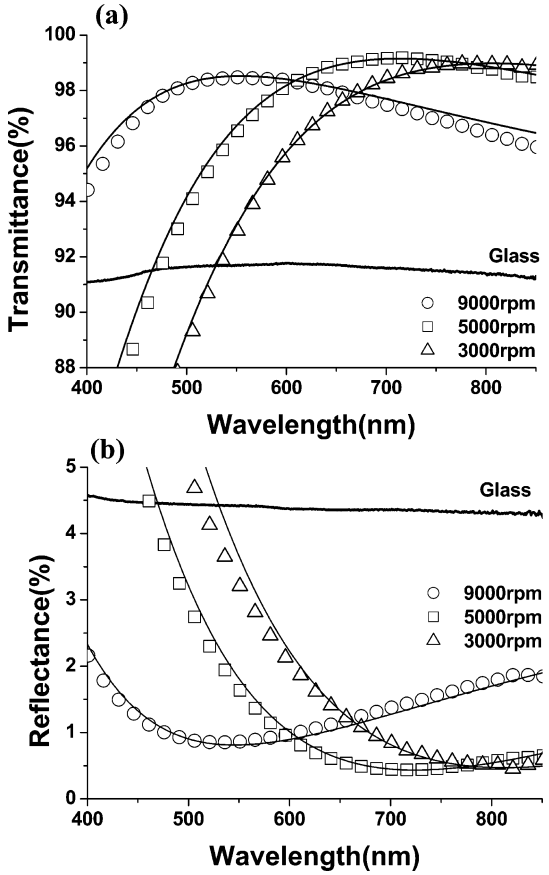

Figure 1. Transmittances (a) and reflectances (b) of glasses spin-coated with PMMA solution (0.009 g/cm^3) in chloroform with 2 vol % of nonane at three rotating speeds [9000 (○), 5000 (□), and 3000 (△) rpm]. The measured ones are shown as symbols, whereas the predicted ones are given as solid lines. For reference, transmittance and reflectance of the glass are added.

transmittance should occur at a wavelength less than 477 nm, which is calculated from $4n_od$ with $n_o = 1.49$ corresponding to pure PMMA film without pores. This is because n of the PMMA film spin-coated from the solution should be lower than 1.49, due to the existence of porous structure in the spin-coated PMMA film. But the wavelength corresponding to the maximum transmittance for this film was 550 nm, as shown in Figure 1a; thus, a one-layer model is not valid for this film. We concluded that the porous morphology of the PMMA film prepared by spin-coating was not uniform in the thickness direction.

Figure 2 shows cross section, top, and bottom images of PMMA films prepared by spin-coating at three different rotating speeds. The cross-sectional images at low magnification (Figure 2A,B,C) and at high magnification (Figure 2a,b,c) showed that PMMA films had two distinct morphologies consisting of a dense skin layer and an inner porous layer. Interestingly, dense skin layers contained small portions of round pores with sizes of 100−200 nm (Figure 2d,e,f). Pore areas in the top of the films were 8.0, 6.8, and 3.5% at 9000, 5000, and 3000 rpm, respectively. Co-continuous porous morphology similar to a thin slice of sponge structure was seen in bottom layers (Figure 2g,h,i).

On the basis of two distinct morphologies, a two-layer film by using the characteristic matrix theory[1] (See Supporting Information) is employed to calculate transmittance

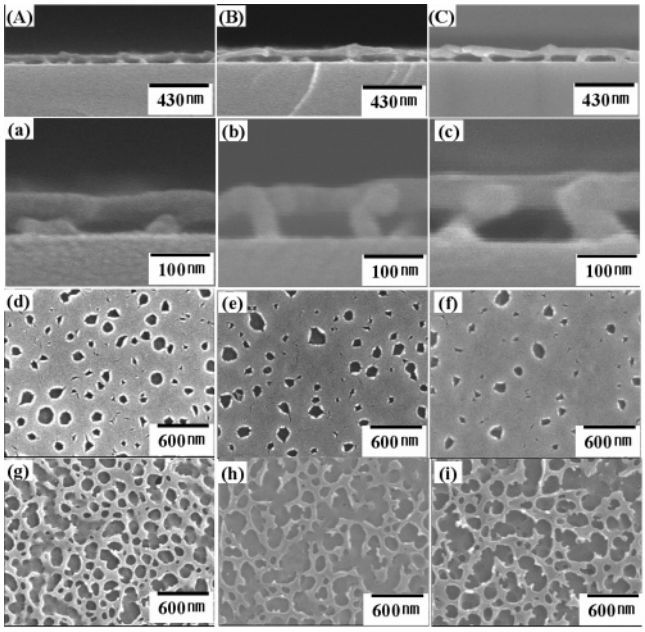

Figure 2. SEM images of cross sections (A, B, C) at low magnification and (a, b, c) at high magnification, and top (d, e, f) and bottom (g, h, i) images of spin-coated PMMA films from 0.009 g/cm^3 PMMA (540K) solution in chloroform with 2 vol % of nonane at three different rotating speeds; (A, a, d, g) 9000 rpm, (B, b, e, h) 5000 rpm, and (C, c, f, i) 3000 rpm.

and reflectance by assuming that light scattering and absorption are negligible. Since the variations in n for PMMA and glass with wavelength in visible region (400−850 nm) were quite small (1.49 ± 0.010 and 1.52 ± 0.006, respectively), n of each layer in the two-layer porous PMMA film was assumed to be constant at the entire wavelengths. Here, the thickness and refractive index of the top layer (d_1, n_1) and those for the bottom layer (d_2, n_2) were adjusted as fitting variables. But, since the total film thicknesses ($d = d_1 + d_2$) for three films were measured by AFM (80 nm for 9000 rpm, 101 nm for 5000 rpm, and 111 nm for 3000 rpm), three parameters [d_1 (or d_2), n_1, n_2] were adjusted to give the best fit to the experimental data. Three films prepared by three rotating speeds were characterized: (1) a top layer with 42 nm and $n = 1.451$ and a bottom layer with 38 nm and $n = 1.230$ for a film prepared under 9000 rpm; (2) a top layer with 56 nm and $n = 1.457$ and a bottom layer with 45 nm and $n = 1.110$ for a film prepared under 5000 rpm; and (3) a top layer with 61 nm and $n = 1.473$ and a bottom layer with 50 nm and $n = 1.100$ for a film prepared at 3000 rpm. Two thicknesses (d_1, d_2) for three films obtained from the characteristic matrix theory are almost the same as those [(42 nm, 35 nm) at 9000 rpm, (56 nm, 48 nm) at 5000 rpm, and (63 nm, 53 nm) at 3000 rpm, respectively] measured by cross-sectional SEM images (Figure 2a−c).

The values of n_1 and n_2 for each film could be estimated from the pore fraction at each layer by using the following relationship[10,26]

$$n_e^2 = n_o^2 \times (1 - \phi) + \phi \qquad (1)$$

where n_e, n_o, and ϕ are the effective refractive indices of

(26) Yoldas, B. E. *Appl. Opt.* **1980**, *19*, 1425.

porous PMMA film and pure PMMA film, and porosity, respectively. Calculated values n of the top layer, with porosities determined from SEM images and $n_o = 1.49$, were 1.457, 1.462, and 1.476 for 9000, 5000, and 3000 rpm, respectively. These values are consistent with those obtained from the characteristic matrix theory. Furthermore, with decreasing rpm, the calculated n value of the top layer increases (namely, a decrease in pore fraction), which is consistent with SEM images (Figure 2d,e,f). Calculated transmittances and reflectances of the films prepared at different rpm are shown as solid lines in Figure 1a,b. The predicted values are in good agreement with measured ones.

We also tried to characterize the films by spectroscopic ellipsometry by assuming two Cauchy layers on the substrate. From the best fit of experimental results, (d_1, n_1) and (d_2, n_2) were obtained (See Supporting Information). However, we found that these values obtained from spectroscopic ellipsometry were not consistent with total film thickness measured by cross-sectional SEM images and n_e obtained from eq 1. This might be attributed to the interface roughness of the porous film.

To measure transmittance and reflectance for AR coating, normal incidence ($\theta = 0°$) was adopted, where path length is the shortest. But, path length increases with increasing angle, which is usually employed for ellipsometric measurement. This suggests that transmittance and reflectance measured at $\theta = 0°$ are less affected by diffusing light than those measured at larger angles. Furthermore, for AR coating with very large transmittance (and very small reflectance), the contribution of diffusing reflectance on transmittance is very small, whereas that on reflectance would not be negligible. For instance, the diffuse reflectance was 0.17% at 550 nm for a porous film prepared at 9000 rpm, whereas transmittance and reflectance were 98.5% and 0.84%, respectively. Thus, in this experiment, we measured total reflectance including specular and diffuse reflectances to measure reflectance more accurately. The good agreement between predicted transmittance and reflectance by the characteristic matrix theory and experimentally measured ones for a film with the roughened interface is because of negligible contribution of the diffusing light to transmittance as well as the measurement of total reflectance.

Interestingly, these two-layer structures with $n_1 > n_2$ have not been reported in the literature. This is because most of the AR effect has been achieved for the two-layer film for $n_1 < n_2$, e.g. $n_1(1.38)/n_2(1.70)$.[1] It is noted that the effectiveness of the AR coating can be determined by the maximum (or minimum) value of transmittance (reflectance) at a given wavelength as well as the range of wavelengths ($\Delta\lambda$) at which higher (or lower) transmittance (reflectance) than that of glass is shown. Minimum reflectance achieved for the two-layer film prepared in this study was very similar to that (0.8−1%) of a commercially available one (for instance, Arctop UR-11 CRNF, Asahi Glass Co.) Also, $\Delta\lambda$ for the two-layer film was broader than that of a commercial two-layer design.

Now, we consider why two distinct morphologies (or asymmetric porous structures) were obtained for PMMA films spin coated on glass. This kind of asymmetric structure was observed in gas separation membranes prepared by a ternary system of polymer/solvent/nonsolvent under dry, wet, and dry/wet phase inversion processes. Pinnau and Koros[19,20] systematically investigated dry, wet, and dry/wet phase inversion processes with polysulfone(PSU)/chlorinated solvents/alcohol nonsolvents. In the dry phase inversion process, solvent and nonsolvent are removed solely by evaporation. They showed that PSU membrane prepared by dry phase inversion process had a very thick dense skin layer and inner porous layer. In the wet phase inversion process, the solution is cast and immediately quenched in nonsolvent. Phase inversion is induced by solvent/nonsolvent exchange. PSU membrane prepared by the wet phase inversion had a defective skin layer and inner porous layer. In the dry/wet phase inversion process, a dense skin layer is generated by evaporation, whereas the inner porous layer is formed by quenching of the membrane in nonsolvent media. They suggested that the dry/wet phase inversion process becomes the best for the fabrication of gas separation membranes with a defect-free dense skin layer and inner porous layer.

The spin-coating of PMMA solution in chloroform with a small amount of nonsolvent of alkanes might be referred to as a dry phase inversion process. For a nonsolvent whose vapor pressure is lower than that of chloroform, chloroform evaporates much faster from the surface of the solution upon spin-coating. Then, the surface of the solution can easily be solidified compared with inner parts of the solution. On the other hand, the alkane content in the inner layer increases with time. The solution at the inner layer then becomes a phase-separated structure consisting of a polymer-rich phase and nonsolvent-rich phase. The latter becomes porous after the complete evaporation of solvent and nonsolvent.

Interestingly, the PMMA films prepared by spin-coating had some pores on the top layer. It is known that an asymmetric membrane prepared by a ternary system contains some defective pores at the top layer.[27,28] Strathmann and Kock[27] showed that the highly defective skin layer (namely, many pores in skin layer) of a membrane prepared under wet phase inversion was due to small macrovoids that were formed from stress-induced rupture of the skin layer by the intrusion of the quench medium. Also, the formation of defective pores on the skin layer is attributed to the incomplete coalescence of polymer.[28] In the case of a spin-coating employed in this study, pores observed at the skin layer of PMMA films was due to the combined effects of phase separation, kinetic effect, and stress-induced rupture. During rapid evaporation of the solvent, the nonsolvent content and consequent viscosity at the top layer would be higher than those in the bottom layer. Then, polymer chains are easily precipitated. The growth of the nonsolvent-rich phase is hampered, and the pore sizes resulting from this phase become smaller. However, the inner layer remains as a fluid for a longer time than the top layer; thus, the size of the phase-separated morphology becomes larger. This is the case where the dense skin layer has a smaller number of pores and smaller pore size compared with those of the inner layer. Finally, stress-induced rupture of the nonsolvent-rich

(27) Strathmann, H.; Kock, K. *Desalination* **1977**, *21*, 241.
(28) Kesting, R. E.; Fritzche, A. K.; Cruse, C. A.; Moore, M. D. *J. Appl. Polym. Sci*. **1990**, *40*, 1575.

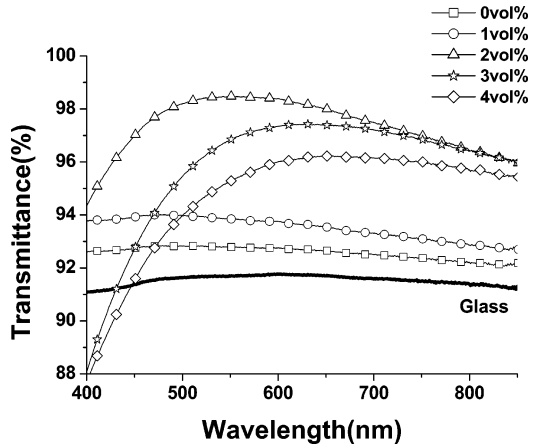

Figure 3. Transmittances of glass spin-coated on both sides with PMMA solution (0.009 g/cm^3) in chloroform with various amounts of nonane at 9000 rpm.

phase existing at the top layer might be a source to generate pores at the top layer. This is because spin-coated film is exposed at higher shear stress resulting from spin-coating as well as very thin thickness compared with a conventional membrane.

It is also noted that the size of pores seen in the top and inner layers was 100−200 nm, which was much smaller than that (ca. micron sized) observed in conventional membranes. Two reasons might be considered. The first is the film thickness. The films prepared in this study had thickness of ∼100 nm, much smaller than that (∼10 μm) in conventional membranes. Thus, the size of the phase-separated domain in a confined geometry becomes smaller. Walheim et al.[29] reported that the size of the dispersed phase in PS/PMMA thin films decreased with decreasing thickness, although the overall morphology was not changed by varying thickness. The second is the kinetic effect, because of fast drying and solidification resulting from spin-coating. The growth of a phase-separated domain needs mobility of polymer chains. Since drying of solvent and nonsolvents during spin-coating causes rapid solidification, the phase-separated domain is not likely to grow to micron size.

We considered the effect of the amount of nonane on the formation of two-layer structures of PMMA films prepared by spin-coating. Figure 3 shows transmittances of PMMA films spin-coated on both sides of glass with various amounts of nonane. The film without nonane became clear, similar to amorphous polymer films prepared by spin-coating with good solvent. Transmittance increased a little (∼1% at 550 nm) compared to uncoated glass because the refractive index of PMMA (1.49) is slightly lower than that of glass (1.52). We do not see any interference color by the naked eye. A glass spin-coated with PMMA film prepared by a solution with 1 vol % of nonane also became clear, and the transmittance was increased by 2.1% at 550 nm compared to uncoated glass. This is because 1 vol % of nonane has some effect on the film morphology. Interestingly, at 2 vol % of nonane, the transmittance of coated glass increases dramatically, as shown in Figure 1. However, with a further

(29) Walheim, S.; Boltau, M. B.; Mlynek, J.; Krausch, G.; Steiner, U. *Macromolecules* **1997**, *30*, 4995.

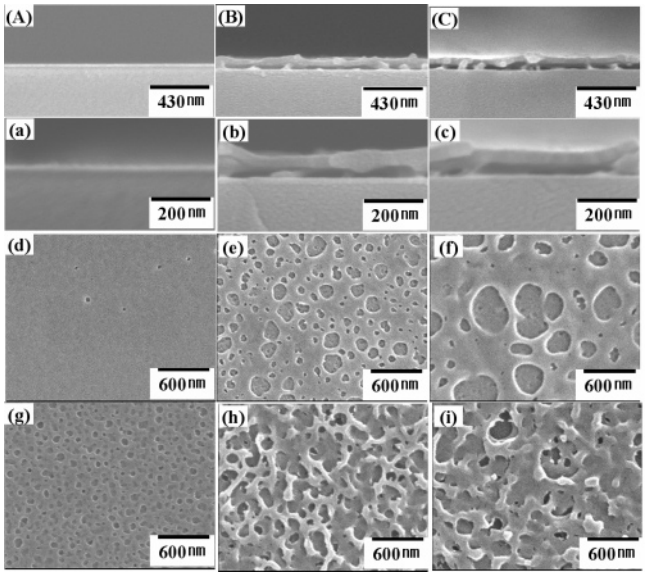

Figure 4. SEM images of cross sections (A, B, C) at low magnification and (a, b, c) at high magnification; top (d, e, f) and bottom (g, h, i) images of spin-coated PMMA films from 0.009 g/cm^3 PMMA (540K) solution in chloroform at three different amounts of nonane at 9000 rpm. The volume fraction of nonane is 1% (A, a, d, g), 3% (B, b, e, h), and 4% (C, c, f, i).

increase in the amount of nonane (3 vol % and higher), the film shows a milky white color, indicating the presence of the scattering of incident light. The transmittance becomes smaller than that prepared with 2 vol % of nonane.

Figure 4 gives SEM images of the cross section, top, and bottom surfaces of PMMA films prepared by using various contents of nonane. Without nonane (data not shown), the top and bottom morphologies of PMMA film are featureless, and the cross-sectional image shows a compact PMMA film. At 1 vol % of nonane, we cannot see two distinct layers in the cross-sectional image of Figure 4A,a. Also, the film surface is flat, but a few defective pores are clearly seen, as shown in Figure 4d. The pore fractions in the bottom of the film (Figure 4g) are much larger than those in the top of the film. We consider that at 1 vol % of nonane, PMMA film has a dense skin layer with pore area less than 2 vol %. When a two-layer model was applied to this film, it is characterized as follows: a top layer with 48 nm and n = 1.49 and a bottom layer with 10 nm and n = 1.35. Therefore, we conclude that 1 vol % of nonane is insufficient to give inner porous layers suitable to high AR layer. As the amount of nonane increases (3 and 4 vol %), film surfaces have more and larger pores (Figure 4e,f). Also, lateral pore sizes in inner layers increased significantly compared to films prepared with 2 vol % of nonane. These pores in the top surface and larger pore sizes located at the inner porous layer induced more scattering of incident light; thus, transmittances decreased.

Since the vapor pressure of the nonsolvent is important to produce an inner porous layer, various alkanes from carbon number six (hexane) to 13 (tridecane) were employed as nonsolvents. Figure 5 gives the transmittance of glasses spin-coated at 9000 rpm on both sides from PMMA solution (0.009 g/cm^3) in chloroform with three different nonsolvents. It was found that for hexane, the transmittance did not increase and spin-coated glass appeared clear without any

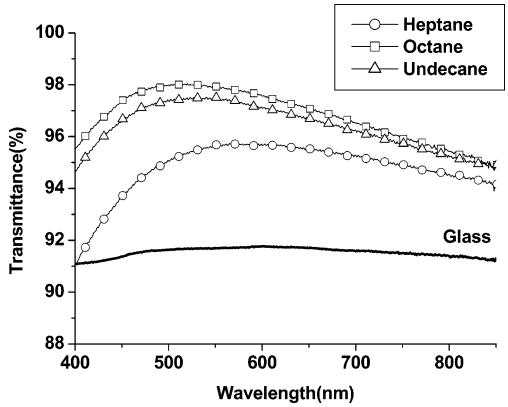

Figure 5. Transmittance of glasses spin-coated at 9000 rpm on both sides from PMMA solution (0.009 g/cm^3) in chloroform with three different nonsolvents: (○) 10 vol % of heptane, (□) 3 vol % of octane, and (△) 1.5 vol % of undecane.

interference color, even when the amount of hexane was increased up to 30 vol %. This suggests that neither macrophase separation nor nanophase separation took place during spin-coating, because the vapor pressure at 25 °C and the boiling point of hexane (20.2 kPa and 69 °C) are very close to those of chloroform (26.2 kPa and 61 °C). However, for heptane with a vapor pressure at 25 °C of 6.09 kPa and a boiling point of 98 °C, the transmittance was 95.7% at 10 vol % of heptane. When 3 vol % of octane (or 1.5 vol % of undecane) was added to PMMA solution in chloroform (0.009 g/cm^3), the transmittances increased to 98% at 520 nm (97.5% at 530 nm). Thus, as the vapor pressure of a nonsolvent decreased, the volume fraction of the nonsolvent corresponding to the maximum transmittance became smaller. This means that nonsolvent with lower vapor pressure (higher boiling point) effectively develops a two-layer structure to be used as a good AR film during spin-coating, even with a smaller amount of a nonsolvent. But for a nonsolvent with lower vapor pressure (for instance, undecane), it would take more time to evaporate the solvent residing in the inner layer below the skin layer; thus, more defects and larger pore size in the inner layer are expected because of increased phase separation times, which caused a slight decrease in the transmittance, as shown in Figure 5.

Compared with conventional porous AR films having rough surface and large air fractions in the top surface, the two-layer structure developed in this study had a skin layer on the top surface. This skin layer could be employed for further functional coating, such as surface modification by a polymer with low surface energy, as long as the solution did not penetrate into the inner porous layer within a short time during further spin-coating. A thin layer of amorphous fluoropolymer (AF) layer was spin-coated on the AR film prepared from 0.009 g/cm^3 in chloroform with 2 vol % of nonane at 9000 rpm. Figure 6a shows transmittances of a glass coated with AF layer onto PMMA film having a two-layered structure. Without the AF layer, the maximum transmittance of 98.5% was observed at 550 nm (see Figure 1a). Even if a thin layer of AF was coated on the two-layer structure of PMMA film, a high transmittance with a maximum transmittance of 98% was maintained. Although the interface of the AF layer and the top layer of PMMA film was not clearly visible in the cross-sectional SEM image,

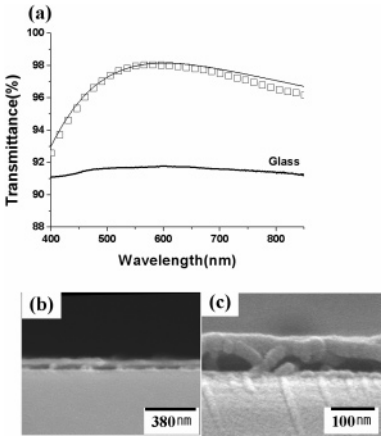

Figure 6. (a) Transmittance of a glass coated with a 10 nm of AF layer onto a two-layer film prepared from PMMA solution (0.009 g/cm^3) in chloroform with 2 vol % of nonane at 9000 rpm. The solid curve is the prediction based on a three-layer model. Cross-sectional SEM images of the PMMA film with a 10 nm AF layer at low magnification (B) and at high magnification (b).

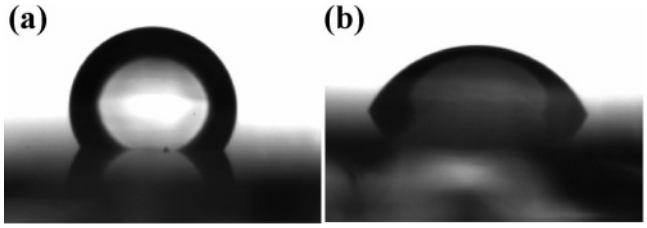

Figure 7. Water droplet shapes on (a) PMMA film with a 10 nm AF layer and (b) PMMA film itself, respectively.

as shown in Figure 6b, the thickness of the AF layer coated on the PMMA AR film was estimated to be 10 nm. This is because the total film thickness was ∼90 nm (Figure 6b,c), and the thickness of the two-layer porous PMMA film was 80 nm (Figure 2a). We also found that when AF solution was spin-coated directly on a silicon wafer under the same condition, the film thickness of AF measured by a spectroscopic ellipsometer (M-2000V, J. A. Woollams Co.) was 10 nm. When a three-layer model, where an additional 10 nm of AF with $n = 1.34$ was added to the same two-layer structure of PMMA as that in Figure 2B,b, was employed, the prediction by the characteristic matrix theory was in good agreement with experimental data. Also, the AF coating did not alter the two-layer structure of the film, as shown in Figure 6B,b. This suggests that the initial two-layer structures, namely thicknesses and refractive indices, were well preserved, and three distinct layers were generated. The reason that the two-layer structures did not change even for additional coating might be due to the very small pore fraction (less than 10%) as well as short residence time for the solution to penetrate into the inner porous layer because of fast spin-coating. Due to the existence of a thin AF layer, the water contact angle was significantly increased to 116° (Figure 7a) from 52° without the AF layer (Figure 7b). Finally, better mechanical properties, such as wear and scratch resistance, might be achieved without sacrificing AR effect, when a polymer with very high molecular weight is coated followed by cross-linking. This will be a subject for future investigation.

Conclusion

We have shown that spin-coating of a polymer/solvent/nonsolvent ternary system on the glass exhibits an excellent AR with a transmittance of over 98% at visible wavelength. This is because of the two-layer structure: a solid skin layer that formed due to fast solvent evaporation during spin-coating and an inner porous layer resulting from phase separation between the polymer-rich phase and a phase rich in solvent including nonsolvent. This one-step process has an advantage in the preparation of AR coating film over conventional methods, which require multistep treatment and/or post-treatment. Furthermore, due to the dense skin layer in this AR film, an additional spin-coating could be easily performed on this film.

Acknowledgment. We thank Dr. Y. S. Kang at KIST for the discussion on the formation of asymmetric morphology and Dr. Y. J. Hong and Mr. Y. Koo at LG Chem, Ltd. for constructive comments. The perfluorinated solvent was kindly supplied by 3M Korea. This work was supported by the Creative Research Initiative Program and the National RND Program for Nano Science and Technology (M1-0214-00-0230).

Supporting Information Available: Measurement of total film thickness by AFM, characterization of a two-layer film by spectroscopic ellipsometry, and procedure for fitting experimental data with characteristic matrix theory. This material is available free of charge via the Internet at http://pubs.acs.org.

CM0500758